Constraints on resonant particle production during inflation from the matter and CMB power spectra

G. J. Mathews,[1,2] D. J. H. Chung,[3] K. Ichiki,[2,4] T. Kajino,[2,4] and M. Orito[5]

[1]*Center for Astrophysics, Department of Physics, University of Notre Dame, Notre Dame, Indiana 46556, USA*
[2]*National Astronomical Observatory, 2-21-1, Osawa, Mitaka, Tokyo 181-8588, Japan*
[3]*Department of Physics, University of Wisconsin, Madison, Wisconsin 53706, USA*
[4]*University of Tokyo, Department of Astronomy, 7-3-1 Hongo, Bunkyo-ku, Tokyo 113-0033, Japan*
[5]*Research Laboratory for Nuclear Reactors, Tokyo Institute of Technology, Meguro-ku, Tokyo 152-8550, Japan*

(Received 21 May 2004; published 4 October 2004)

We analyze the limits on resonant particle production during inflation based upon the power spectrum of fluctuations in matter and the cosmic microwave background. We show that such a model is consistent with features observed in the matter power spectrum deduced from galaxy surveys and damped Lyman-α systems at high redshift. It also provides an alternative explanation for the excess power observed in the power spectrum of the cosmic microwave background fluctuations in the range of $1000 < l < 3500$. For our best-fit models, epochs of resonant particle creation reenter the horizon at wave numbers of $k_* \sim 0.4$ and/or 0.2 (h Mpc^{-1}). The amplitude and location of these features correspond to the creation of fermion species of mass $\sim 1 - 2$ M$_{pl}$ during inflation with a coupling constant between the inflaton field and the created fermion species of near unity. Although the evidence is marginal, if this interpretation is correct, this could be one of the first observational hints of new physics at the Planck-scale.

DOI: 10.1103/PhysRevD.70.083505 PACS numbers: 98.80.Cq, 98.80.Es, 98.65.Dx

I. INTRODUCTION

Analysis of the power spectrum of fluctuations in the large-scale distribution of matter (cf. [1–3]), together with fluctuations in the cosmic microwave background (CMB) (cf. [4]) provides powerful constraints on the physics of the very early universe. The most popular account for the origin of both power spectra is based upon quantum fluctuations generated during the inflationary epoch [5]. Subsequently, acoustic oscillations of the photon-baryon fluid distort this to produce the observed features in the angular power spectrum of temperature fluctuations in the CMB and the spatial power spectrum of matter density fluctuations. The two power spectra are different in that the cosmic microwave background is sensitive to the baryonic material, while the matter power spectrum probes the dominating dark matter.

In this context, there now exist determinations of the matter power spectrum on small angular scales due to recent SDSS [2,6], and 2dF [7] galaxy surveys as well as analysis of the Lyman-α forest [8,9] at higher redshift and even smaller scales. This latter determination is particularly facilitated by the fact that at high redshift, the Lyman-α absorption systems are still within the quasi-linear regime so that an inference of the primordial power spectrum is relatively straightforward. The overall matter power spectrum deduced in this way is consistent with a standard ΛCDM cosmology, but as shown in Fig. 1 there is marginal evidence of a peculiar feature beginning near $k \sim 0.6\ h\,\mathrm{Mpc}^{-1}$ which is not easily explained away by systematic errors [9]. There is also at least a possibility for structure to exist in the region near $k \sim 0.3\ h\,\mathrm{Mpc}^{-1}$. In this paper we consider that such features may be a part of the primordial spectrum generated by new physics near the end of the inflation epoch.

Regarding the CMB, data [10] from WMAP have placed stringent constraints on the cosmological parameters relevant to the observed power spectrum in the range of multipoles up to $l \leq 1000$. The simplest prediction of the standard ΛCDM cosmology is that the primordial

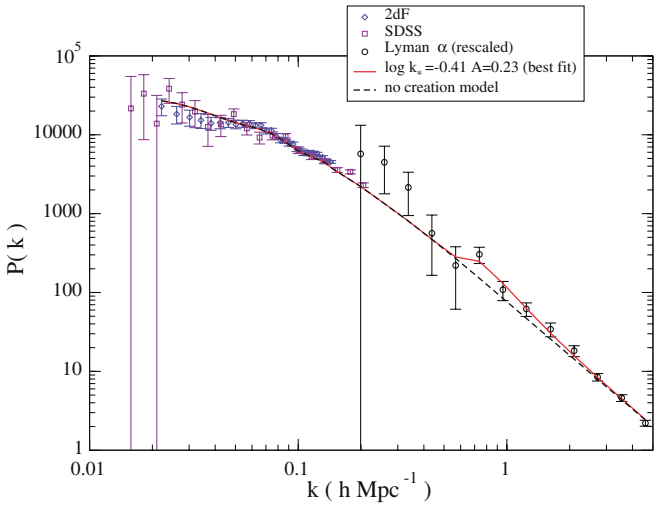

FIG. 1 (color online). Comparison of the observed galaxy cluster function from SDSS [6], 2dF [7], and Lyman-α [8] with the spectrum implied from the fits to the matter power spectrum with (solid line) and without (dashed line) resonant particle creation during inflation as described in the text.

power spectrum should be strongly damped at higher multipoles due to photon diffusion (Silk damping) and because more than one perturbation can fit within the depth of the surface of last scattering, and hence, be washed out.

Of interest for the present work, however, is the recent accumulation of observations of the CMB power spectrum in the range $1000 < l < 7000$ by various groups (CBI [11–13], ACBAR [14], BIMA [15], and VSA [16]). These observations on the smallest angular scales are of particular interest as a test of this basic prediction of the standard inflation/photon-decoupling paradigm. The current data are summarized in Fig. 2 from which it is clear that the deduced power spectrum increases rather than decreases for large multipoles, particularly in the range $2000 < l < 3500$.

The most likely interpretation (cf. [17,18]) of an excess power at high multipoles is a manifestation of the scattering of CMB photons by hot electrons in clusters known as the thermal Sunyaev-Zeldovich (SZ) effect [19]. Although some contribution from the SZ effect undoubtedly occurs, it is not yet conclusively established that this is the only possible interpretation (cf. [20]) of excess power on small angular scales. Indeed, it has been deduced [17,18] that explaining the excess power in the observed CMB spectrum requires that the mass density fluctuation amplitude parameter, σ_8, be near the upper end of the range of the values deduced via other independent means. Another significant effect is the large cosmic variance. The uncertainties on the SZ contribution are highly non-Gaussian. They thus depend strongly upon whether or not the observed field happens to contain a group or cluster of galaxies. Hence, there is large uncertainty in any deduced SZ effect. In view of these uncertainties, an exploration of other possible explanations for this power excess seems warranted.

Indeed, alternative explanations exist for the generation of features in both the matter and CMB power spectra on small angular scales. For example, a flattening of the inflation generating effective potential near the end of inflation could produce such distortions on small angular scales [21].

In this paper, however, we consider another alternative originally proposed in [22] whereby such distortions might arise from the resonant production of particles during large field inflation.[1] This interpretation has the intriguing aspect that, if correct, an opportunity emerges to use the CMB and matter power spectra as probes of the Planck-scale ($M_{pl} \sim 10^{19}$ GeV) particle spectrum.

The prototypical scenario is that there is an inflaton ϕ which controls the mass of a fermion ψ or a boson χ

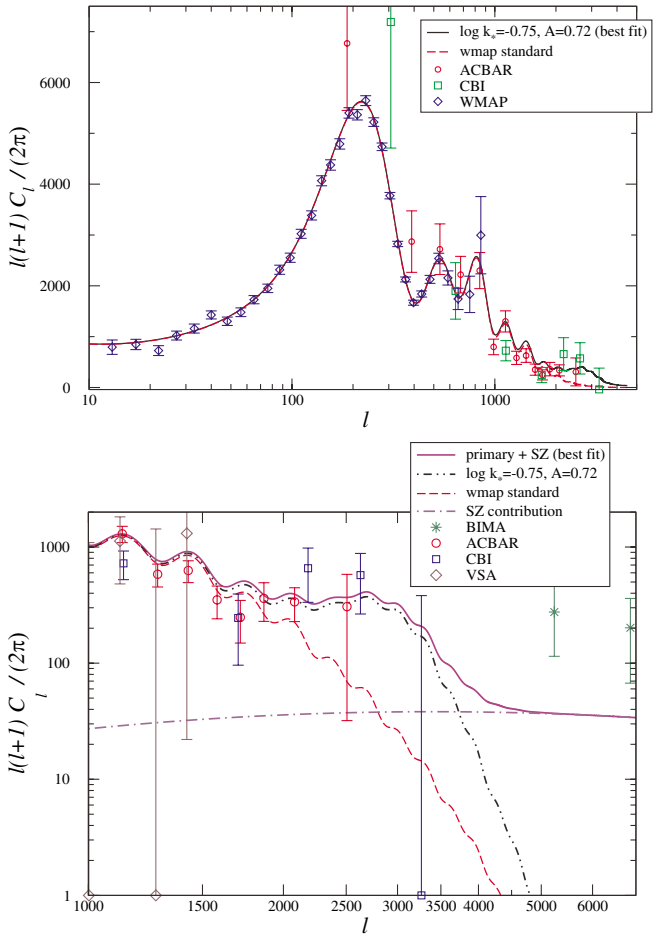

FIG. 2 (color online). Upper figure shows the CMB, WMAP, ACBAR, and CBI data in the range $l = 10$–5000. The dashed line is the CMB power spectrum computed using the standard WMAP cosmological parameters. The thick solid line is for a best-fit to these data for a model with resonant particle production included. The lower figure shows an expanded view of the ACBAR, CBI, VSA, and BIMA data in the range of $l = 1000$–7000. The dashed line shows the standard WMAP result without the SZ effect included. The dot-dashed line shows our fit SZ contribution (from the analytic halo model of Ref. [18]). The solid line shows the best-fit to these data sets with resonant particle production and the SZ effect included. The dot-dot-dashed line shows the resonant particle creation component without the SZ contribution.

through the coupling

$$L_{\rm int} = -\left[M_f - M_{pl} f\left(\frac{\phi}{M_{pl}}\right)\right]\bar{\psi}\psi - \left[M_B^2 - M_{pl}^2 g\left(\frac{\phi}{M_{pl}}\right)\right]\chi^2, \quad (1)$$

where M_f and M_B are fermion and boson masses, respectively, which are assumed to be of order M_{pl}. Since by the definition of large field inflationary scenario $\phi/M_{pl} \gtrsim 1$ and ϕ/M_{pl} varies at least an order of magnitude, any

[1]Large field inflation is a slow-roll inflationary scenario in which the inflaton scalar field has a classical field value exceeding the Planck scale.

natural order unity functions $f(x)$ and $g(x)$ will lead to a cancellation of the masses during the evolution of slow-roll inflation. Because of this cancellation, when $|M_f - M_{pl}f| \lesssim H$ and/or $|M_B - M_{pl}g| \lesssim H$, the effective-mass of ψ and χ is varying nonadiabatically (since the inflaton field variation time rate is also typically not too far from the Hubble expansion rate H).[2] During this nonadiabatic period, there is efficient particle production which can be thought of as a kind of resonant particle production.

In [22], the effect of the resonant *fermionic* particle production was taken into account neglecting the nonadiabatic effects on the modes outside of the horizon. This leads to a bumplike structure in the primordial power spectrum. However, [23] considered the nonadiabatic effects of bosonic particle production on the modes outside the horizon. Their claim is that the primordial power spectrum is modified to a steplike structure rather than a bumplike structure. Given that their analysis was for bosonic particle production while we are going to deal with fermionic production following [22],[3] and given that the subtle effect of [23] (which was only approximately computed numerically) requires more detailed attention to unambiguously establish the change in the qualitative behavior of the primordial spectral feature, we will in this paper consider only the semianalytic results of [22] when fitting to data. However, because of this omission of the nonadiabatic effect, this result should only be considered indicative of the type of constraints one can obtain from the latest data. A detailed analysis of the nonadiabatic effects will be considered in a future publication.

Planck-scale-mass particles generically exist in Planck-scale compactification schemes of string theory from the Kaluza-Klein states, winding modes, and the massive (excited) string modes. Hence, the existence of Planck-scale-mass particles which couple to the inflaton is a generic situation. What is perhaps not generic in the scenario considered in this paper is that the mass of the Planck-scale particle lies in the e-fold range of the inflaton accessible to observation.

Even with all of these favorable assumptions, we find only marginal hints for the existence of such a particle from fits to current data. More specifically, we find marginal hints for a bump at a scale of $k \sim 0.4$ (and 0.2) h Mpc^{-1} in the primordial spectrum due to production of fermions of mass $m \approx 2M_{pl}$ with an O(1) weak coupling to the inflaton.

The order of presentation will be as follows. In section II, we briefly review and clarify the semianalytic results of [22] and then set up the parametrization of the primordial spectrum fitting function. In sections III and IV, we briefly discuss the matter power spectrum parametrization and the CMB power spectrum (including the SZ effect which is the more conservative interpretation of the excess power at large l values). Section V is devoted to the discussion of the fitting procedure and the fit results to the matter and the CMB spectrum. Finally, we conclude in section VI.

II. INFLATION RESONANT PARTICLE PRODUCTION

In the basic inflationary picture, a rapid early expansion of the universe is achieved through the vacuum energy from an inflaton field. In the minimal extension from the basic picture considered here, the inflaton is postulated to couple to at least one massive particle whose mass is order of the of the inflaton field value. This particle is then resonantly produced as the field obtains a critical value during inflation. If even a small fraction of the energy in the inflaton field is extracted in this way, it can produce features in the primordial power spectrum. In particular, there will be excess power in the spectrum at the angular scale corresponding to when the epoch of resonant particle creation crossed the Hubble radius.

In the simplest slow-roll approximation [5] for the generation of density perturbations during inflation, the amplitude, $\delta_H(k)$, of a density fluctuation when it crosses the Hubble radius is just,

$$\delta_H(k) \approx \frac{H^2}{5\pi\dot{\phi}}, \tag{2}$$

where H is the expansion rate, and $\dot{\phi}$ is the velocity of the inflaton field when the comoving wave number k crosses the Hubble radius during inflation. If resonant particle production drains energy from the inflaton field, then the conjugate momentum in the field $\dot{\phi}$ decreases. This causes an increase in $\delta_H(k)$ (primordial power spectrum) for those wave numbers which exit the horizon during the resonant particle production epoch.

Of course when $\dot{\phi}$ is changing due to particle production, $\ddot{\phi}$ may not be negligible, resulting in corrections to Eq. (2). In [22], this correction was considered and found to be $<< 20\%$[4] for the particle production of interest for the fits of this paper.

[2]More precisely, for quadratic monomial inflaton potentials, the nonadiabaticity condition $\frac{\dot{w}_k}{w_k^2} > 1$ leads approximately to

$$H > y(M_f - M_{pl}g)$$

for fermion mass term where

$$y = \frac{4\pi|g^{-1}(M_f/M_{pl})|}{|g'|}\left(\frac{M_f}{M_{pl}} - g\right).$$

[3]Dealing with fermionic particle production allows us to avoid dealing with nonminimal phase transition effects that can arise due to the possible nontrivial ground states of the bosonic field.

[4]This fraction refers to the fraction of the particle production effect, not the entire power spectrum amplitude.

The inflaton field is then postulated to have a simple Yukawa coupling to a fermion field ψ of mass m in the form,

$$\mathcal{L}_Y = -\lambda\phi\bar{\psi}\psi. \tag{3}$$

Including this new coupling, the equation of motion for the inflaton field becomes

$$\ddot{\phi} + 3H\dot{\phi} + \frac{dV}{d\phi} - N\lambda\langle\bar{\psi}\psi\rangle = 0, \tag{4}$$

for N fermions of mass m coupled to the inflaton. The effective-mass of the fermion is $M(\phi) = m - \lambda\phi$, which vanishes for a critical value of the inflaton field, $\phi_* = m/\lambda$. Resonant fermion production will then occur in a narrow range of inflaton field amplitude around $\phi = \phi_*$.

As in [22] we label the epoch at which particles are created by an asterisk. So the cosmic scale factor is labeled a_* at the time t_* at which resonant particle production occurs. Considering a small interval around this epoch, one can treat $H = H_*$ as approximately constant (slow-roll inflation). The number density n of particles can be taken as zero before t_* and afterwards as $n = n_*[a_*/a(t)]^3$. The fermion vacuum expectation value can thus be written,

$$\begin{aligned}\langle\bar{\psi}\psi\rangle &\approx n_*\theta(t - t_*)[a_*/a(t)]^3 \\ &\approx n_*\theta(t - t_*)\exp[-3H_*(t - t_*)].\end{aligned} \tag{5}$$

Now inserting this relation into the equation of motion for the inflaton field (Eq. (4)), one can obtain the change in the inflaton field evolution $\dot{\phi}$ due to particle creation,

$$\begin{aligned}\dot{\phi}(t > t_*) = \phi(t > t_*)_{\lambda=0} + N\lambda n_*\theta(t - t_*) \\ \times\exp[-3H_*(t - t_*)].\end{aligned} \tag{6}$$

Inserting this into Eq. (2), a very good analytic approximation to the effect of the particle creation on the perturbation spectrum can be obtained [22],

$$\delta_H(k) = \frac{[\delta_H(k)]_{\lambda=0}}{1 - \theta(a - a_*)|\dot{\phi}_*|^{-1}N\lambda n_* H_*^{-1}(a_*/a)^3\ln(a/a_*)}. \tag{7}$$

The scale factor a relates [24] to the physical wave number k by,

$$\begin{aligned}\ln\frac{k}{a_0H_0} = 62 + \ln\left[\frac{a}{a_*}\right] + \ln\left[\frac{a_*}{a_{\rm end}}\right] - \ln\frac{10^{16}\ {\rm GeV}}{V_k^{1/4}} \\ + \ln\frac{V_k^{1/4}}{V_{\rm end}^{1/4}} - \frac{1}{3}\ln\frac{V_{\rm end}^{1/4}}{\rho_{\rm reh}^{1/4}},\end{aligned} \tag{8}$$

where $a_0H_0 \approx (h/3000)\ {\rm Mpc}^{-1}$ denotes the present comoving Hubble scale. The subscript "k" indicates the inflaton effective potential value when a particular wave number k crosses the Hubble radius during inflation ($k = aH$). The quantities $a_{\rm end}$ and $V_{\rm end}$ are the scale factor and effective inflaton potential at the end of inflation, and $\rho_{\rm reh}$ is the matter energy density after reheating to the standard hot big bang Friedmann cosmology. This expression assumes that instantaneous transitions occur between the various regimes, and that the universe behaves as if matter-dominated during reheating.

Using this relation between scale factor and k, the perturbation spectrum (Eq. (7)) can be reduced [22] to a simple two-parameter function.

$$\delta_H(k) = \frac{[\delta_H(k)]_{\lambda=0}}{1 - \theta(k - k_*)A(k_*/k)^3\ln(k/k_*)}, \tag{9}$$

where the coefficient A and characteristic wave number k_* ($k/k_* \geq 1$) can be fit to the observed power spectra. (Note that this A is *different* from the A coefficient of [22].)

The values of A and k_* determined from observation directly relate to the inflaton coupling λ and fermion mass m, for a given inflation model. When the back reaction is not important, we can write

$$A = |\dot{\phi}_*|^{-1}N\lambda n_* H_*^{-1} \tag{10}$$

which uses the approximation [22,25–27] for the particle production Bogoliubov coefficient to be

$$|\beta_k|^2 = \exp\left(\frac{-\pi k^2}{a_*^2\lambda|\dot{\phi}_*|}\right). \tag{11}$$

Note that this approximation does not depend on the particular form of the inflaton potential. Its main assumptions are only that the particle mass being produced is nearly negligible during the resonant production (which is an excellent assumption for our case) and that the effective-mass time variation due to the inflaton time variation dominates over the contribution due to the FRW expansion. Hence, when we carry out the fits, we can approximately marginalize over the spectral index (since each constant spectral index corresponds to a different inflationary model in which the spectral index is approximately constant).

The coefficient A in this approximation of negligible back reaction can be related directly to the coupling constant λ by noting that

$$n_* = \frac{2}{\pi^2}\int_0^\infty dk_p k_p^2|\beta_k|^2 = \frac{\lambda^{3/2}}{2\pi^3}|\dot{\phi}_*|^{3/2}. \tag{12}$$

This gives us

$$A = \frac{N\lambda^{5/2}}{2\pi^3}\frac{\sqrt{|\dot{\phi}_*|}}{H_*} \tag{13}$$

$$\approx \frac{N\lambda^{5/2}}{2\sqrt{5}\pi^{7/2}}\frac{1}{\sqrt{\delta_H(k_*)|_{\lambda=0}}} \tag{14}$$

where we have used the usual approximation for the primordial slow-roll inflationary spectrum [5]. This

means that regardless of the exact nature of the inflationary scenario, for any fixed inflationary spectrum $\delta_H(k)|_{\lambda=0}$ without the back reaction, we have the particle production giving us a bump of the form Eq. (9) with the parameter A expressed in terms of the coupling constant through Eq. (14). Given that the CMB normalization requires $\delta_H(k)|_{\lambda=0} \sim 10^{-5}$, we have

$$A \sim 1.3N\lambda^{5/2}. \tag{15}$$

Hence, for $A \sim O(0.1)$, both $\lambda < 1$ and $\lambda N < 1$ are possible, satisfying perturbativity. As will be seen in the sections below, our best fits will indeed give $A \sim O(0.1)$. When N and λ are sufficiently large that the back reaction becomes important (when the naively computed $A \sim O(3)$),[5] the back reaction reduces [22] the actual amplitude of the peak relative to the perturbative value given by Eq. (14).

Before we conclude this section, we would like to explicitly state further caveats to using Eq. (2) in computing the primordial perturbation spectrum:

(1) Instead of the usual long wavelength gauge invariant curvature perturbation variable implicit in using Eq. (2), the gauge invariant gravitational potential must be recomputed incorporating the coupling of Eq. (3).
(2) Even with the usual gauge invariant curvature perturbation formalism, Eq. (2) neglects the change in pressure that occurs due to the particle production. Even considering the adiabatic perturbation component, this would change the denominator of Eq. (2).
(3) The numerator of Eq. (2) also obtains a contribution from the particle production which we are neglecting.
(4) As pointed out by [23], perhaps the most significant effect that has been neglected is the nonadiabatic pressure change.

A more detailed investigation of these neglected effects will be deferred to a future publication.

III. MATTER POWER SPECTRUM

It is straightforward to determine the matter power spectrum to compare with that deduced from large-scale structure surveys [6,7] and the Lyman-α forest [8]. To convert the amplitude of the perturbation as wave number k enters the horizon, $\delta_H(k)$, to the present day power spectrum, $P(k)$, which describes the amplitude of the fluctuation at a fixed time, one must make use of a transfer function, $T(k)$ [28] which is easily computed using the code CMBFAST [29] for various sets of cosmological parameters (e.g. Ω, H_0, Λ, Ω_B). An adequate approximate expression for the structure power spectrum is

$$\frac{k^3}{2\pi^2}P(k) = \left(\frac{k}{aH_0}\right)^4 T^2(k)\delta_H^2(k). \tag{16}$$

This expression is only valid in the linear regime, which in comoving wave number is up to approximately $k \lesssim 0.2\ h\,\mathrm{Mpc}^{-1}$ and therefore adequate for our purposes. However, we also correct for the nonlinear evolution of the power spectrum [30].

IV. CMB POWER SPECTRUM

Features in the primordial power spectrum will also appear in the observed CMB temperature fluctuations. The connection between the resonant particle creation and CMB temperature fluctuations is straightforward. As usual, temperature fluctuations are expanded in spherical harmonics, $\delta T/T = \sum_l \sum_m a_{lm} Y_{lm}(\theta, \phi)$ ($2 \leq l < \infty$ and $-l \leq m \leq l$). The anisotropies are then described by the angular power spectrum, $C_l = \langle |a_{lm}|^2 \rangle$, as a function of multipole number l. One then merely requires the conversion from perturbation spectrum $P(k)$ to angular power spectrum C_l. This is also easily accomplished using the code CMBFAST [29]. As input to CMBFAST we adopt the usual power law primordial spectrum plus the perturbation due to resonant particle production. For speed, CMBFAST does not compute all C_l, but uses a spline fit to interpolate. We have checked the stability of the CMBFAST results when adding such features to the power spectrum by increasing the number of C_l explicitly computed. The results were convergent even for the default spline fits of CMBFAST. When converting to the angular power spectrum, the amplitude of the narrow particle creation feature in $\delta_H(k)$ is spread over many values of l. Hence, the particle creation feature looks like a broad peak which is easily accommodated even when implementing spline fits.

A. SZ effect

It has been proposed [17,18] that the observed spectrum at high l is explained by the SZ effect. However, the amplitude of the SZ contribution to the power spectrum is very sensitive to the parameter σ_8 describing rms mass fluctuation within a fiducial 8 h^{-1} Mpc sphere. The amplitude of the expected SZ peak scales as σ_8^7.

Explaining the excess power in the observed CMB spectrum requires that the mass density fluctuation amplitude parameter, σ_8, be slightly above unity [18]. However, a variety of independent measures including weak lensing [31], galaxy velocity fields [32], galaxy clusters at high redshift [33], X-ray emitting clusters [34], and the independent value obtained by the WMAP fit [10] to the lower multipole data all favor a mean value in the range $\sigma_8 \sim 0.7 - 0.9$ (see Ref. [17] for a recent review). Note that even a slight reduction of the amplitude parameter by 10% is sufficient to reduce the magnitude of distortion by more than a factor of 2. For the present

[5]The back reaction becomes very strong as $A \to 3e \approx 8$.

purposes we adopt a conservative value of $\sigma_8 = 0.9 \pm 0.1$ as a reasonable prior distribution based upon the various independent measures of σ_8.

In what follows we fit the amplitude of the SZ contribution using the SZ power spectrum calculated in [18] based upon the analytic halo formalism [35]. This analytic form has been shown [17,18] to adequately represent the power spectra deduced from numerical simulations.

V. RESULTS

We have made a multidimensional Markov Chain Monte-Carlo analysis [36,37] of the mass power spectrum based upon the combined 2df, SDSS, and Lyman-α data in models with and without resonant particle creation during inflation to alter the primordial fluctuation spectrum. We also have independently analyzed the CMB using the combined WMAP, CBI, ACBAR, and VSA data. In addition, we made a total analysis based upon the combined mass and CMB power spectra.

For simplicity and speed in the present study we only marginalized over the five parameters which do not alter the matter or CMB transfer functions. Hence, the set of free parameters in the analysis is $(n_s, A_s, \log(k_*), A, A_{SZ})$, where n_s is the spectral index, A_s is the overall amplitude of the primordial power spectrum, and A_{SZ} is the overall amplitude of the SZ effect which we relate to an effective σ_8^{SZ} parameter for the SZ effect. The true σ_8 parameter, however, is determined by A_s once the power spectrum and transfer functions are fixed. As usual, both n_s and A_s are normalized at $k = 0.05$ Mpc^{-1}. As noted above, we adopt a conservative prior of $\sigma_8^{SZ} = 0.9 \pm 0.1$ as opposed to the best-fit combined WMAP analysis value of $\sigma_8 = 0.84 \pm 0.04$. For this illustrative study all other parameters for this analysis were fixed at the optimum WMAP parameters [10], i.e., $(h, \Omega_b h^2, \Omega_m h^2, \Omega_\Lambda, \tau) = (0.71, 0.0224, 0.135, 0.75, 0.17)$. One expects that different results would arise by optimizing over other parameters, e.g. $h, \Omega_b h^2$, etc., However, for the present exploratory study, we only wish to identify angular scales which might be of interest for future study. For this purpose, a simple five parameter marginalization is adequate since such parameters do not produce the kind of spectrum bump of interest here.

A. Matter power spectrum fit

Contours of constant goodness of fit in the A vs. k_* plane consistent with the matter power spectrum constraint are shown on Fig. 3. These fits are based upon the 2dF, SDSS, and Lyman-α data described above. Window functions required for fits to these data sets are given in approximate analytic form in [7] for the 2dF data, and in [6] for the SDSS data. As described in [38], a simple χ^2 is used to fit for the Lyman-α data, because the full correlation matrix is not available.

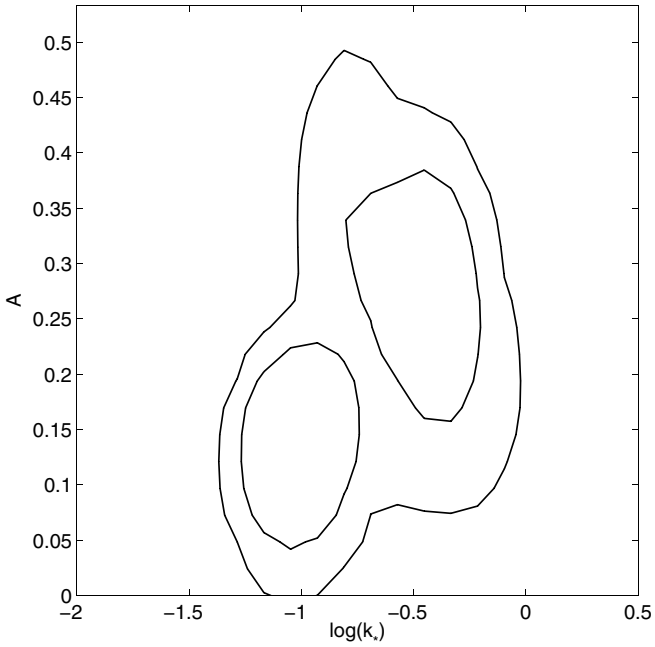

FIG. 3. Constrains on parameters A and k_* from the fit to the matter power spectrum alone. Contours show one and two σ confidence limits. The horizontal axis indicates $\log(k_*)$ where k_* is in units of (h Mpc^{-1}).

The most recent SDSS matter power spectrum extends into the nonlinear regime, but is probably not reliable [2] for the last band widths above $k = 0.2\ h\,\mathrm{Mpc}^{-1}$. Hence, we have omitted the last points of the SDSS for $k \geq 0.2\ h\,\mathrm{Mpc}^{-1}$ and for $k \geq 0.15\ h\,\mathrm{Mpc}^{-1}$ for the 2dF power spectrum as recommended [2]. For the SDSS and 2dF power spectra the unknown bias factors (multiplier to get from the matter power spectrum to the galaxy power spectrum) were analytically marginalized according to the method described in the appendix of Ref. [37].

The contours on Fig. 3 identify two possible regions which could be consistent with resonant particle production. The feature with the largest amplitude occurs at $k_* = 0.41 \pm 0.05\ h\,\mathrm{Mpc}^{-1}$ and with $A = 0.23 \pm 0.08$. These parameters correspond to $m \approx 2.2\ \mathrm{M}_{pl}$ and $\lambda \approx 0.6$ for a single fermion species.

The weaker feature has a minimum at $k_* = 0.08 \pm 0.01\ h\,\mathrm{Mpc}^{-1}$ and an amplitude $A = 0.12 \pm 0.04$. This feature is more or less consistent with a similar feature seen in the CMB, but at a lower amplitude and slightly larger angular scales. This feature would correspond to $m \approx 1.8\ \mathrm{M}_{pl}$ and $\lambda \approx 0.5$. However, it occurs at the interface between the SDSS and Lyman-α power spectra, and hence, may be an artifact of the matching of the data sets rather than a real bump in the spectrum. Obviously, this is another feature which warrants further careful scrutiny.

Figure 1 shows the effect of the stronger feature on the matter power spectrum compared with data from 2dF,

SDSS, and Lyman-α. Clearly the feature in the matter power spectrum beginning near $k \approx 0.6\ h\,\mathrm{Mpc}^{-1}$is important in this regard and warrants careful scrutiny. (Note that the peak of the primordial spectrum bump generically occurs at $k \approx \exp(1/3)k_*$ with our parametrization.)

B. CMB Fit

Cosmological parameters with and without resonant particle creation were obtained from the combined WMAP, CBI, ACBAR, and VSA data using a Markov chain Monte-Carlo analysis [36] as described above. Figure 4 shows the one and two σ contours in the k_* vs A plane from this analysis. The CMB power spectrum is best-fit for $A = 0.7 \pm 0.2$ and $k_* = 0.18 \pm 0.02\ h\,\mathrm{Mpc}^{-1}$.

Figure 2 shows our best-fit to the CMB data for models with and without resonant particle creation. Also shown for comparison in the lower expanded figure is the SZ contribution for $\sigma_8 = 0.9$. We find that an excellent fit to the ACBAR and CBI observed CMB power spectra can be achieved in this way. Indeed, those CMB observations favor this interpretation over the conventional SZ plus ΛCDM models at the level of 5σ. However, the *BIMA* data set at $l \approx 5000$–7000 is a crucial test of this possible interpretation. If the power spectrum is as high at these l-values as the BIMA data imply, then an SZ interpretation with a large σ_8 is favored.

C. Combined Analysis

Contours of A and k_* consistent with the combined CMB and matter power spectrum constraints are shown on Fig. 5. Here it is apparent that a single feature which begins in the matter power spectrum at $k_* = 0.17 \pm 0.04\ h\,\mathrm{Mpc}^{-1}$ and has an amplitude of $A \approx 0.35 \pm 0.10$ is most prominent. Figure 6 illustrates the associated optimum fits to the matter power spectrum (upper curve) and the CMB (lower curve).

As remarked above, even though a feature with $k_* \sim 0.2$ appears in both the matter and CMB power spectra, it is not unambiguously attributable to resonant particle production. In the matter power spectrum it could be an artifact of the uncertainty in joining of the galaxy and Lyman-α data sets near $k \approx 0.1$, while in the CMB its significance could be confused by the SZ effect. Nevertheless, the feature with $k_* = 0.4\ h\,\mathrm{Mpc}^{-1}$ and $A \approx 0.2$ which is clearly seen in the matter power spectrum of Fig. 1 is still apparent in the combined analysis. The diminished significance in the combined analysis is to be expected since this bump is entirely due to the Lyman-α data and is not detectable in the CMB.

Regarding other parameters in the analysis, it is not surprising that we deduce values very near to the WMAP [10] optimum results, e.g., $n_s = 0.96 \pm 0.01$, $\sigma_8 = 0.88 \pm 0.08$.

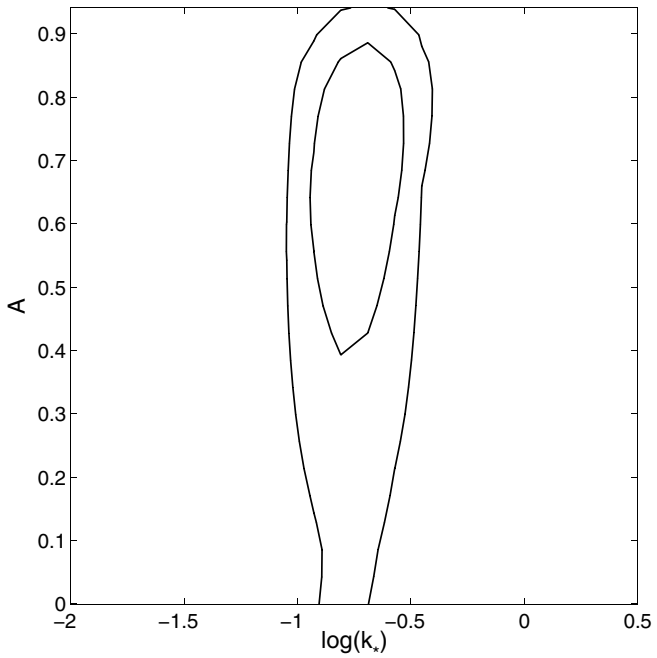

FIG. 4. Constrains on parameters A and k_* from the CMB power spectrum. Contours show one and twoσ limits. The horizontal axis indicates $\log(k_*)$ where k_* is in units of (h Mpc^{-1}).

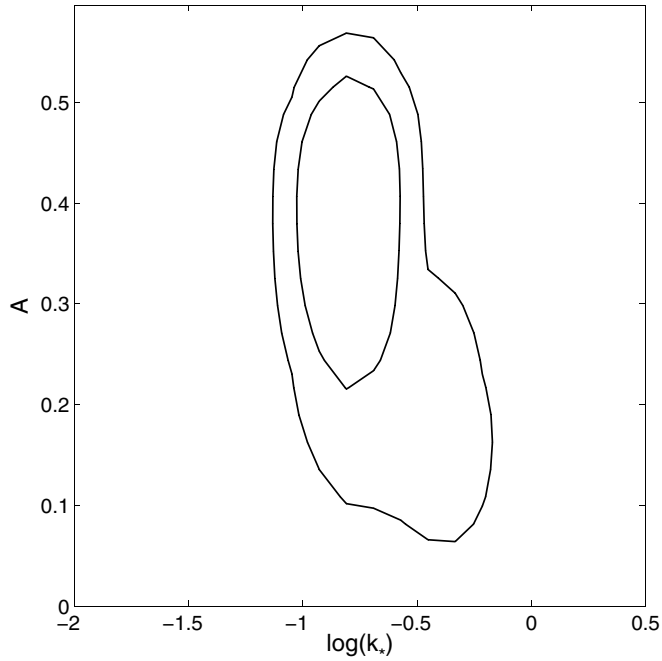

FIG. 5. Constrains on parameters A and k_* from a fit to the combined CMB and matter power spectra. Contours show one and 2σ limits. The horizontal axis indicates $\log(k_*)$ where k_* is in units of (h Mpc^{-1}).

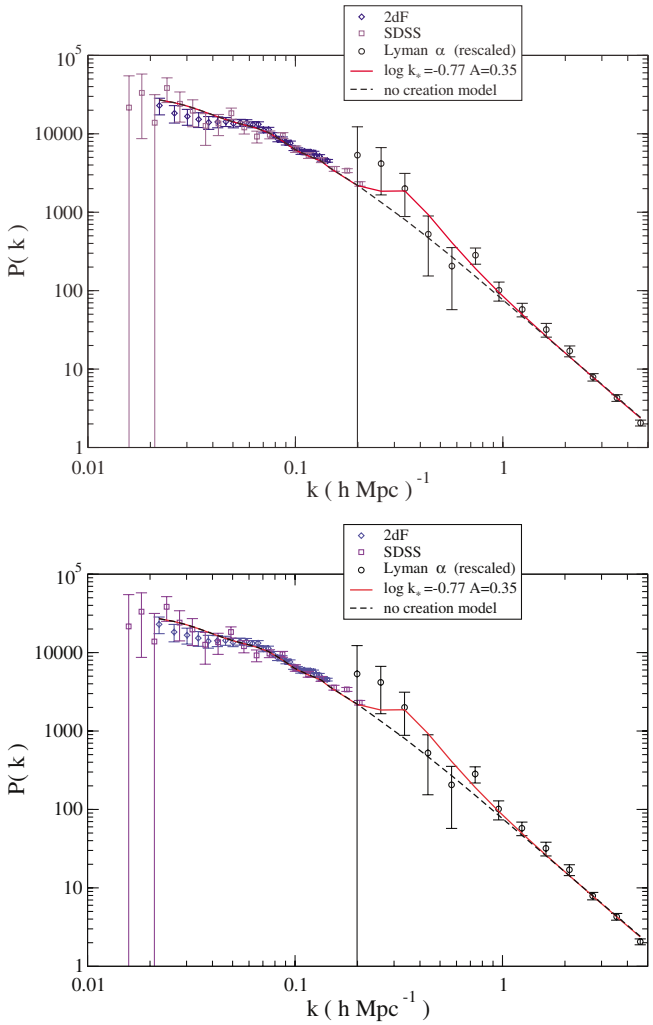

FIG. 6 (color online). Optimum fit to the combined CMB + matter power spectra. Upper figure shows the observed galaxy cluster function from SDSS [6], 2dF [7], and Lyman-α [8] data. The solid line shows the spectrum implied from the optimum model with resonant particle creation during inflation. The lower figure shows an expanded view of the ACBAR, CBI, VSA, and BIMA data in the range of $l = 1000$–7000. The dashed line shows the standard WMAP result without the SZ effect included. The solid line shows the optimum fit with resonant particle production and the SZ contribution. The dot-dot-dashed line shows the resonant particle creation component without the SZ effect.

VI. CONCLUSION

We have analyzed the mass and CMB power spectra in the context of a model for particle creation during inflation. We find marginal evidence for excess power in both the CMB and mass fluctuation spectra consistent with this hypothesis. The combined CMB + matter power spectrum would imply an optimum feature at $k_* = 0.17 \pm 0.04\ h\,\mathrm{Mpc}^{-1}$ and $A \approx 0.35 \pm 0.10$. However, given that the CMB results may be attributed to the SZ effect and that the matter power spectrum is very uncertain at this scale, we propose that the most likely possibility could be the feature in the matter power spectrum deduced from the Lyman-α absorption structures at a scale of $k \sim 0.4\ h\,\mathrm{Mpc}^{-1}$ and $A \approx 0.2$. Either of these features would correspond to the resonant creation of a particle with $m \approx 1$–$2\ \mathrm{M}_{pl}$ and a Yukawa coupling constant between the fermion species and the inflaton of $\lambda \approx 0.5 - 1.0$ for a single fermion species.

Obviously there is a need for more precise determinations of the primordial matter power spectrum on the scale of 0.1–10 Mpc. Indeed, the Lyman-α forest constraints and method are currently under revision and new results are expected shortly which may alter the conclusions presented here. There is also a need for more precise determinations of the SZ contribution to the CMB on the scale of $l \approx 2000$–$10\,000$. We further note that the present analysis has neglected the possibility of nonadiabatic effects. Based upon previous studies [39,40] of nonadiabatic isocurvature fluctuations on the matter power spectrum and CMB, we would expect that the introduction of non-Gaussian isocurvature fluctuations could add excess power on small angular scales and hence could decrease the significance of the features identified here. They would not, however, naturally produce the kind of bump of interest here, and hence would not easily explain such features away.

In spite of these caveats, we conclude that if the present analysis is correct, this may be one of the first hints at observational evidence of new particle physics at the Planck-scale. Indeed, one expects a plethora of particles at the Planck-scale, particularly in the context of string theory, the leading candidate for a consistent theory of quantum gravity. Perhaps, the presently observed power spectra contain the first suggestion that such particles may have not only existed in the early universe, but coupled to the inflaton field, and thereby, left a relic signature of their existence in the primordial power spectrum.

ACKNOWLEDGMENTS

Work at the University of Notre Dame is supported by the U.S. Department of Energy under Nuclear Theory Grant No. DE-FG02-95-ER40934. This work has been supported in part by the Grants-in-Aid for Scientific Research (12047233, 13640313, 14540271) and for Specially Promoted Research (13002001) of the Ministry of Education, Science, Sports, and Culture of Japan.

[1] M. Tegmark, M. Zaldarriaga, and A. J. S. Hamilton, Phys. Rev. D **63**, 043007 (2001).
[2] M. Tegmark *et al.*, Astrophys. J. **606**, 702 (2004).
[3] A. J. Hamilton and M. Tegmark, Mon. Not. R. Astron. Soc. **330**, 506 (2002).
[4] W. Hu, D. Scott, N. Sugiyama, and M. White, Phys. Rev. D **52**, 5498 (1995).
[5] E.W. Kolb and M. S. Turner, *The Early Universe*, (Addison-Wesley, Menlo Park, 1990).
[6] SDSS Collaboration, S. Dodelson *et al.*, Astrophys. J. **572**, 140 (2002); M. Tegmark, A. J. S. Hamilton, and Y. Xu, Mon. Not. R. Astron. Soc. **335**, 887 (2002).
[7] 2dF Collaboration, W. Percival *et al.*, Mon. Not. R. Astron. Soc. **328**, 1039 (2001).
[8] R. A. Croft *et al.*, Astrophys. J. **581**, 20 (2002).
[9] N. Y. Gnedin and A. J. S. Hamilton, Mon. Not. R. Astron. Soc. **334**, 107 (2002).
[10] WMAP Collaboration, C. L. Bennett *et al.*, Astrophys. J. Suppl. Ser. **148**, 97 (2003); D. L. Spergel *et al.*, Astrophys. J. Suppl. Ser. **148**, 175 (2003).
[11] CBI Collaboration, B. S. Mason *et al.*, Astrophys. J. **591**, 540 (2003).
[12] CBI Collaboration, T. J. Pearson *et al.*, Astrophys. J. **591**, 556 (2003).
[13] A. C. S. Readhead *et al.*, Astrophys. J.(to be published).
[14] ACBAR Collaboration, C. L. Kuo *et al.*, Astrophys. J. **600**, 32 (2004).
[15] BIMA Collaboration, K. S. Dawson *et al.*, Astrophys. J. **581**, 86 (2002).
[16] VSA Collaboration, K. Grainge *et al.*, Mon. Not. R. Astron. Soc. **341**, L23 (2003).
[17] J. R. Bond *et al.*, astro-ph/0205386 .
[18] E. Komatsu and U. Seljak, Mon. Not. R. Astron. Soc. **336**, 1256 (2002).
[19] R. Sunyaev and Ya. B. Zel'dovich, Mon. Not. R. Astron. Soc. **190**, 413 (1980); Annu. Rev. Astron. Astrophys., **18**, 537 (1980).
[20] N. Aghanim, K. M. Gorski, and J.-L. Puget, Astron. Astrophys. **374**, 1 (2001).
[21] H. Kurki-Suonio, F. Graziani, and G. J. Mathews, Phys. Rev. D **44**, 3072 (1991).
[22] D. J. H. Chung, E.W. Kolb, A. Riotto, and I. I. Tkachev, Phys. Rev. D **62**, 043508 (2000).
[23] O. Elgaroy, S. Hannestad and T. Haugboelle, J. Cosmol. Astropart. Phys. 09 (2003) 008.
[24] A. R. Liddle and D. H. Lythe, *Cosmological Inflation and Large Scale Structure*, (Cambridge University Press, Cambridge, 1998).
[25] N. D. Birrell and P. C.W. Davies, *Quantum Fields in Curved Space*, (Cambridge Univ. Press, Cambridge, 1982).
[26] L. Kofman, A. Linde and A. A. Starobinsky, Phys. Rev. D **56**, 3258 (1997).
[27] D. J. H. Chung, Phys. Rev. D **67**, 083514 (2003).
[28] G. P. Efstathiou, in *Physics of the Early Universe*, edited by A. T. Davies, A. Heavens, and J. Peacock (SUSSP Publications, Edinburgh, 1990).
[29] U. Seljak and M. Zaldarriaga, Astrophys. J. **469**, 437 (1996).
[30] J. A. Peacock and S. J. Dodds, Mon. Not. R. Astron. Soc., **280**, L19 (1996).
[31] H. Hoekstra *et al.*, Astrophys. J. **577**, 604 (2002); A. Refregier, J. Rhodes, and E. J. Groth, Astrophys. J. **572**, L131 (2002); M. L. Brown *et al.*, Mon. Not. R. Astron. Soc. **341**, 100 (2003); M. Jarvis *et al.*, Astron. J. **125**, 1014 (2003); D. Bacon *et al.*, Mon. Not. R. Astron. Soc. **344**, 673 (2003).
[32] J. A. Willick and M. A. Strauss, Astrophys. J. **507**, 64 (1998).
[33] N. Bahcall and P. Bode, Astrophys. J. **588**, L1 (2003).
[34] A. Voevodkin and A. Vikhlinin, Astrophys. J. **601**, 610 (2004).
[35] S. Cole and N. Kaiser, Mon. Not. R. Astron. Soc. **233**, 637 (1988); N. Makino and Y. Suto, Astrophys. J. **405**, 1 (1993); A. Cooray, Phys. Rev. D **62**, 103506 (2000).
[36] N. Christensen, R. Meyer, L. Knox, and B. Luey, Classical Quantum Gravity **18**, 2677 (2001).
[37] A. Lewis and S. Bridle, Phys. Rev. D **66**, 103511 (2002).
[38] WMAP Collaboration, L. Verdi *et al.*, Astrophys. J. Suppl. Ser., **148**, 195 (2003).
[39] N. Sugiyama, S. Zaroubi, and J. Silk, astro-ph/0310593.
[40] R. Trotta, A. Riazuelo, and R. Durer, Phys. Rev. D **67**, 063520 (2003).